STRUCTURE AND MAGNETISM OF A LINEAR TETRANUCLEAR NICKEL COMPLEX LIGATED BY COMPARTMENTAL LIGAND

Feng Zhang[1], Yun Chen[1], Jia-Nan Feng[1], Jian-Hua Sun[1*] and Ching-Cheng Huang[2,3*]

[1]School of Chemistry and Chemical Engineering, Institute of Advanced Functional Materials for Energy, Jiangsu University of Technology, Changzhou 213001, Jiangsu Province, China
[2]Department of Biomedical Engineering, Ming-Chuan University, Taoyuan 333, Taiwan
[3]PARSD Biomedical Material Research Center, Changzhou 213000, China

ABSTRACT. A new nickel(II) complex $[Ni_4L_3(acac)_2(H_2O)_2]\cdot2DMF\cdot Et_2O$ (**1**) (acac = acetylacetonate, and DMF = N,N'-dimethylformamide) was isolated in solid crystalline form with the reaction of nickel(II) acetylacetonate and compartmental Schiff base ligand 1,2-bis(2-hydroxy-3-methoxybenzylidene) hydrazine (H_2L). Single crystal X-ray analysis showed that the complex has a linear tetranuclear structure. In the complex, an unusual μ_3- and μ_4-bridging modes of Ligand L^{2-} were coexisting. Variable-temperature magnetic studies revealed that weak antiferromagnetic interaction exists between the nickel(II) ions coupling through phenoxide$-$O atoms and $-N-N-$ bridging moieties.

**KEY WORDS**: Nickel complex, Linear tetranuclear cluster, Crystal structure, Magnetic properties

INTRODUCTION

Interest in rational design and synthesis of polynuclear coordination complexes of $3d$ metals has increased staggeringly in the field of molecular magnets [1, 2]. Compared to other $3d$ transition metals, nickel ion, $3d^8$ system is often characterised by large magnetic anisotropy leading to production of single-molecule magnets [3]. Within regulating fine structures, huge energy gaps and very large values for the axial zero-field splitting parameter are available in Ni^{2+} complexes [4]. Therefore, numerous of polynuclear nickel complexes presenting a variety of topology structures have been prepared for studying their magnetic properties [5-8].

In general, formation of polynuclear complexes mainly depends on the ligand rational design and their coordination behavior [9]. With specific coordination sites capable of selective binding pockets, compartmental ligands are good candidates to synthesize polynuclear metal complexes [10]. In this regard, plenteous documents are available on the synthesis of compartmental ligands and their polynuclear complexes as the prototype [11, 12]. As a member of the compartmental ligands, 1,2-bis(2-hydroxy-3-methoxybenzylidene) hydrazine (H_2L) with different chelation sites (Scheme 1) coordinates to various metal ions resulting in polynuclear metal complexes [13]. For instance, a Dy_4 single-molecule magnet with a record anisotropic barrier was found in 2009 [14]. Subsequently, a dodecanuclear heterometallic dysprosium–cobalt wheel exhibits single-molecule magnet behavior [15]. And a Gd_5Mn_2 pyramidal complex presents multifunctional luminescent magnetic cryocooler [16]. Consequently, inspired by this, we would like to design and fabricate novel polynuclear nickel(II) clusters and provide insights into their magneto-structure correlation with this ligand. Herein, we used H_2L and nickel ion as the start materials for preparation of a polynuclear complex $[Ni_4L_3(acac)_2(H_2O)_2]\cdot2DMF\cdot Et_2O$ (**1**) (L = 1,2-bis(2-hydroxy-3-methoxy benzylidene) hydrazine, acac = acetylacetonate, and DMF= N,N'-dimethylformamide). In this work, we report the synthesis, structure and magnetic properties of complex **1** in details.

_____
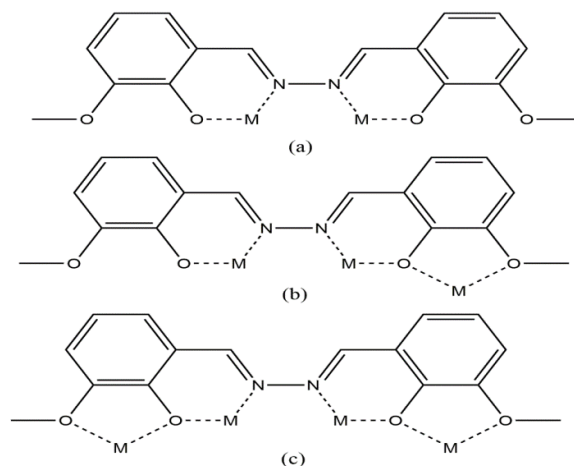
Scheme 1. Bridging modes of the ligand in documents.

EXPERIMENTAL

Materials and methods

All chemicals were of reagent grade and used as received from commercial sources (Shanghai Aladdin Biochemical Technology Co., Ltd) without further purification. Ligand 6,6′-((1,1′)-hydrazine-1,2-diylidenebis(methanylylidene)) bis(2-(6-methoxy)) phenol (H_2L) was prepared according to the literature procedures [17]. Elemental analysis for carbon, hydrogen, and nitrogen were carried out with a Vario EL-III elemental analyzer. Variable-temperature magnetic susceptibility measurement was taken at an applied field of 1 kOe on a Quantum Design MPMS-XL7 SQUID magnetometer working in 300–2.0 K temperature range. Diamagnetic corrections were applied by using Pascal's constants.

Synthesis of $[Ni_4L_3(acac)_2(H_2O)_2]\cdot2DMF\cdot Et_2O$ (1)

To a stirred suspension of H_2L (0.122 g, 0.4 mmol) in DMF (8 mL) was added solid nickel(II) acetylacetonate (1.285 g, 0.5 mmol) to give a deep green solution. After stirring for one hour, the resulting solution was filtered. Green block crystals of **1** suitable for X-ray single-crystal diffraction analysis were obtained (0.297g, 64% yield based on Ni) by slow vapor diffusion of Et_2O into the filtrate over one week. Elemental analyses Calcd. for $C_{68}H_{82}N_8Ni_4O_{21}$ (%): C, 51.62; H, 5.22; N, 7.08. Found: C, 51.36; H, 5.15; N, 7.14.

X-Ray crystallography

The well-shaped single crystal of **1** was selected for X-ray diffraction study. Data collections were performed with graphite-monochromatized Mo Kα radiation ((λ = 0.71073 Å) on a Bruker Smart Apex-II CCD diffractometer, using the φ-ω scan technique. Data reduction was made with the Bruker SAINT package [18]. Absorption correction was performed using the SADABS program [19]. The structure was solved by direct methods and refined by full-matrix least-squares on F^2 with SHELXTL-2018 program package [20]. All non-hydrogen atoms were refined anisotropically, and hydrogen atoms were located and included at their calculated position. The absolute configuration was refined as an inversion twin. Crystallographic data and details on refinements are summarized in Table 1. Selected bond distances and angles are listed in Table 2.

Table 1. Crystallographic data and structure refinement for complex **1**.

Complex	**1**
Temperature (K)	110(2)
Formula	$C_{68}H_{82}N_8Ni_4O_{21}$
Formula weight	1582.25
Crystal system	Orthorhombic
Space group	*Pbcn*
a (Å)	27.905(6)
b (Å)	15.505(3)
c (Å)	16.516(4)
α (deg)	90
β (deg)	90
γ (deg)	90
V (Å^3)	7146(3)
Z	4
Dc (g cm^{-3})	1.471
μ (mm^{-1})	1.117
F (000)	3304
Limiting indices	-30 ≤ h ≤ 30, -17 ≤ k ≤ 17, -18 ≤ 1 ≤18
Reflections collected / unique	41775 / 4960
Data / restraints / parameters	41775 / 4960
R_{int}	0.0591
GOF	1.027
R1[a], wR2[b] [I>2σ(I)] (I)	0.0322, 0.0761
R_1, wR_2 (all data)	0.0443, 0.0832
Largest diff. peak and hole	0.439 and -0.210 e.A^{-3}

[a] $R_1 = \sum ||F_o|-|F_c||/\sum |F_o|$. [b] $wR_2 = [\sum w(|F_o^2|-|F_c^2|)^2/\sum w(|F_o^2|)^2]^{1/2}$.

Table 2. Selected bond lengths (Å) and angles [°] for complex.

Complex **1**					
Ni1—O2	2.012(2)	Ni1—O3	2.001(2)	Ni1—O5^i	2.083(2)
Ni1—N1	2.061(2)	Ni1—N2	2.073(2)	Ni1—N3	2.086(2)
Ni2—O3	1.981(2)	Ni2—O4	2.250(2)	Ni2—O5	2.103(2)
Ni2—O7	2.003(2)	Ni2—O8	1.979(2)	Ni2—O9	2.060(2)
O3—Ni1—O2	90.25(9)	O3—Ni1—N1	178.04(9)	O2—Ni1—N1	87.80(8)
O3—Ni1—N2	85.16(9)	O2—Ni1—N2	94.83(9)	N1—Ni1—N2	94.81(9)
O3—Ni1—O5	79.02(8)	O2—Ni1—O5	88.69(8)	N1—Ni1—O5	101.12(8)
N2—Ni1—O5	163.82(8)	O3—Ni1—N3	94.86(9)	O2—Ni1—N3	171.36(9)
N1—Ni1—N3	87.11(9)	N2—Ni1—N3	92.55(9)	O5—Ni1—N3	85.45(8)
O8—Ni2—O3	178.31(9)	O8—Ni2—O7	91.00(1)	O3—Ni2—O7	90.43(1)
O8—Ni2—O9	91.47(9)	O3—Ni2—O9	87.00(9)	O7—Ni2—O9	172.57(9)
O8—Ni2—O5	101.76(8)	O3—Ni2—O5	79.00(8)	O7—Ni2—O5	95.05(9)
O9—Ni2—O5	91.31(8)	O8—Ni2—O4	104.21(9)	O3—Ni2—O4	74.99(8)
O7—Ni2—O4	86.57(1)	O9—Ni2—O4	86.02(9)	O5—Ni2—O4	153.95(8)
Ni2—O3—Ni1	104.40(9)	Ni1—O5—Ni2	97.48(8)		

RESULTS AND DISCUSSION

*Crystal structure of **1***

From single-crystal X-ray structural analysis, complex **1** crystallizes in the orthorhombic *Pbcn* space group with *Z* = 4. The complex consists of a tetranuclear nickel cluster arranged in linear through the combination of crystallographic independent unit and its symmetry inversion.

Illustrated with atomic numbering in Figure 1, the asymmetric unit contains two Ni^{2+} ions, three half ligands L^{2-}, one acetylacetonate anion, one coordinated water molecule, and three lattice solvents (two DMF and one ether molecules). In the crystal structure of complex **1**, all nickel ions are six coordinated octahedral geometries. The inner Ni1 metal ion was coordinated with three imine–N atoms and three deprotonated phenoxide oxygen atoms from three ligands. In the slightly distorted octahedron of Ni1 (*cis*-angles range from 79.02(8) to 101.12(8)°, and *trans*-angles from 163.82(8) to 178.04(9)°) (Table 2), four atoms (N1, N2, O3 and O5) locate on the sites of equatorial plane, while O2 and N3 occupy the axial positions, with the corresponding bond distances in the range of 2.012(2)–2.086(2) Å (Table 2). On the contrary, the terminal Ni2 ions was satisfied by two oxygen atoms of one acac anion, one coordinated water molecule, two deprotonated phenoxide O atoms and one O-atom of one –OCH$_3$ group of two different molecules of the ligand, respectively. Three oxygen atoms of L^{2-} and one oxygen atom of acac constitute the equatorial plane of the severely distorted octahedral geometry (*cis*-angles range from 74.99(8) to 104.21(9)°, and *trans*-angles from 153.95(8) to 178.31(9)°) of Ni2, whereas the other oxygen atom of acac anion and water molecule sit on the axial positions. The Ni2–O bond lengths fall in the range of 1.981(2) to 2.103(2) Å, comparing to those in other nickel complexes [21].
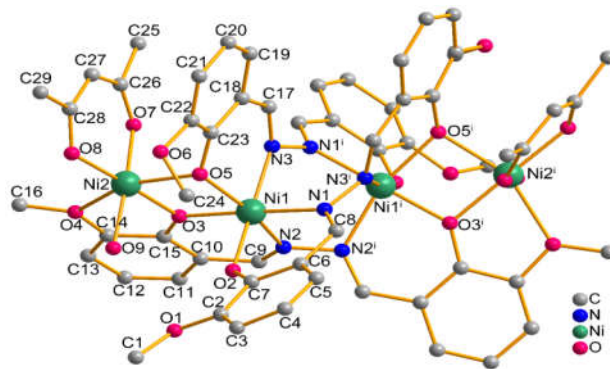

Figure 1. Molecular structure and coordination environment of complex **1**. Hydrogen atoms and solvent molecules have been omitted for clarity; Symmetry codes: [i] -x+1, y, -z+1/2.

For its different chelation sites, the ligand L^{2-} can represent several possible coordination modes. It is interesting that two coordination modes of L^{2-} were observed in complex **1** (Figure 2), never appeared in its complexes. One ligand L^{2-}(N1-N3[i]) displays a rare coordination mode of μ_3–η^1:η^1:η^1:η^2 (Figure 2a), different from the reported coordination modes [13-17]. Whilst, the other one L^{2-}(N2-N2[i]) shows a μ_4–η^1:η^2:η^1:η^1:η^2:η^1 bridging mode (Figure 2b), same as the mode in references [22]. With the μ_3- and μ_4-modes, four nickel ions are linked alternately through two phenoxide oxygen atoms and three −N−N− bridging moieties, resulting in a linear tetranuclear metallic core (Figure 3a). The Ni−O−Ni bond angles are 97.48(8) and 104.40(9)°, which is the critical parameter for magnetic-exchange [23]. Meanwhile, the Ni−N−N−Ni torsion angles are 51.01(6) and 57.87(6)°. The intermetallic Ni···Ni distances are 3.143(6) and 3.582(2) Å, shorter than those in the literature copper and iron complexes [17, 24]. Owning to the two phenoxide−O bridges, Ni1 and Ni2 form a binuclear unit. In the tetranuclear core, both the binuclear Ni(II) centers are truncated at two different planes, and the angle between two equatorial plane is 57.86(8)° (Figure 3b).
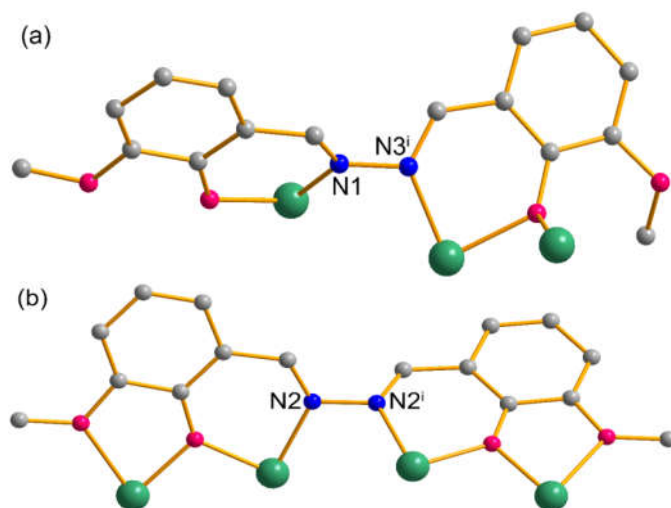
Figure 2. Coordination modes of ligand in complex **1**. (a) μ_3–mode and (b) μ_4–mode. Symmetry codes: [i] -x+1, y, -z+1/2.
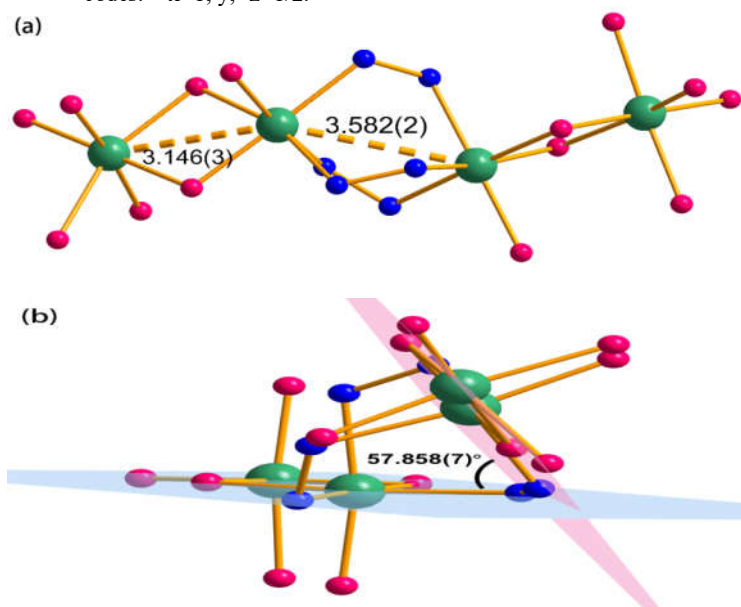

Figure 3. (a) Metallic core and (b) illustrating angle between the equatorial plane of binuclear Ni(II) centers.

In the solid state of complex **1**, the tetranuclear clusters are interlinked though π–π stacking of the phenyl rings from the L^{2-} ligands and weak hydrogen bonds to form a 3D supramolecular structure (Figure 4).
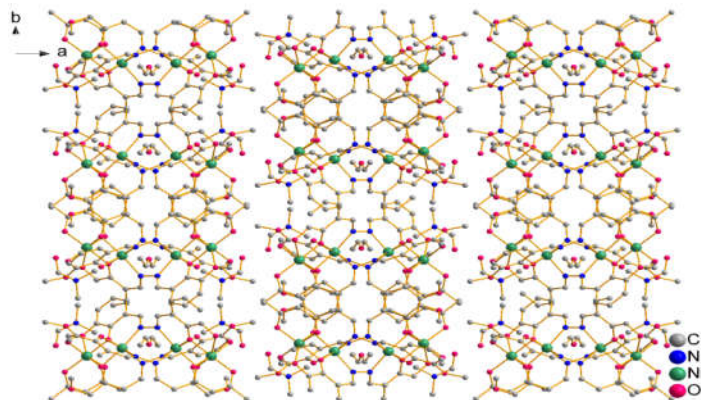
Figure 4. 3D supramolecule structure of **1** along *c* direction. For clearity, hydrogen atoms are deleted.

Magnetic properties

Attributing to the fascinating magnetic behaviors of nickel compounds, we investigated the magnetic properties of complex **1**. At the temperature ranging from 2.0 to 300 K, the direct-current magnetic susceptibility measurements of polycrystalline sample of **1** were performed on a Quantum Design MPMS-XL7 SQUID magnetometer under an applied magnetic field of 1000 Oe. The magnetic measurement results in the form of $\chi_M T$ and χ_M^{-1} versus T are depicted in Figure 5. At room temperature, the $\chi_M T$ value of **1** is 4.75 emu K mol^{-1}, which is slightly higher than the anticipated spin-only value for four non-interacting nickel(II) ions [25]. When the temperature is lowered, the $\chi_M T$ product remains almost constant until 100 K. Upon further cooling, the $\chi_M T$ plot undergoes a decrease abruptly, to reach a minimum value of 0.56 emu K mol^{-1} at 2.0 K, suggesting intramolecular antiferromagnetic coupling between the four Ni^{2+} ions within the linear tetranuclear [26]. Above 30 K, we used the Curie–Weiss law to fit the magnetic susceptibility, giving a Curie constant C = 4.87(2) emu K mol^{-1} and a negative Weiss constant θ = -7.5(8) K. The negative θ value indicates that antiferromagnetic coupling occurs in **1** [27]. To further inspect the magnetic behavior of **1**, isothermal magnetization was conducted in the magnetic field of 0−7 T and at a temperature of 1.8 K. As shown in Figure 6, the field dependence of the magnetization of **1** shows linear behavior in whole fields, as expected for paramagnets [28]. A maximum magnetization value is 2.96 Nβ at 1.8 K and 7 T, much lower than calculated value of 8 Nβ for four Ni^{2+} ions (g = 2), also suggesting that antiferromagnetic coupling happened between nickel ions [29].

Typically, the M−O−M (M = metal) bond angle in the range ~93−98° exhibits ferromagnetic interaction and below or above that range, antiferromagnetic interaction takes place [12]. Here in complex **1**, the Ni−O−Ni bond angles are 97.48(8) and 104.40(9)°, implying that antiferromagnetic interaction exists in Ni1 and Ni2 through two phenoxide oxygen bridges. Simultaneously, the Ni2−N−N−Ni2 (Symmetry codes: -x+1, y, -z+1/2) dihedral angles are in the range of 51−58°, which is far low than 90°. Generally, a dihedral angle close to 90° represents ferromagnetic interactions owing to perpendicular orientation [24]. Therefore, antiferromagnetic interaction is expected for complex **1**, coinciding with the experiment data.
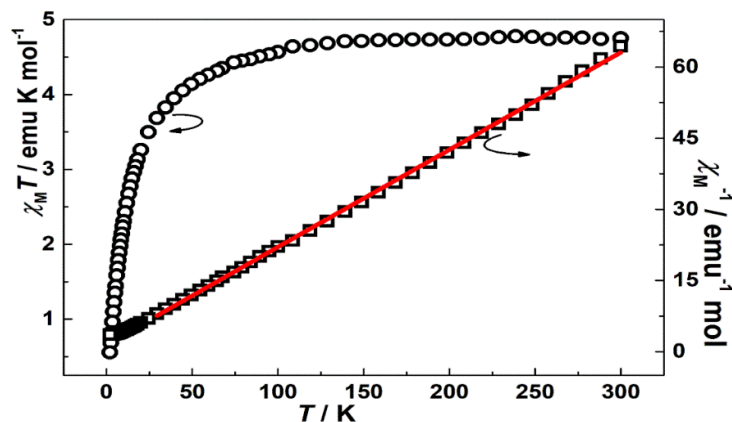
Figure 5. Plots of $\chi_M T$ and χ_M^{-1} vs T for **1**. Solid line represents the best fit of the data with Curie–Weiss law.
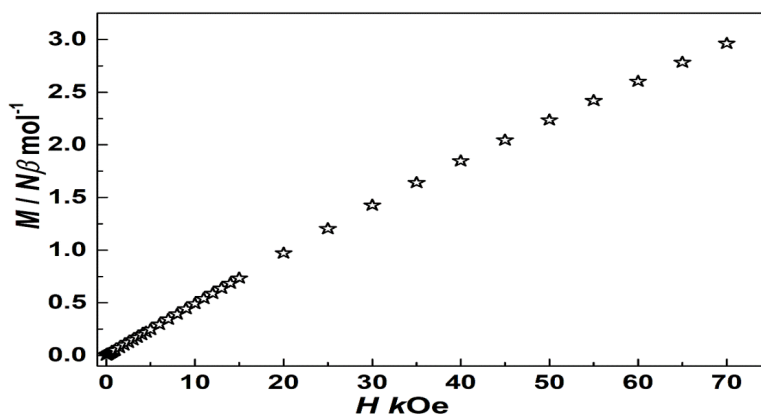

Figure 6. Isothermal magnetization plot of complex **1** at 1.8 K.

CONCLUSION

In summary, a new nickel(II) cluster complex $[Ni_4L_3(acac)_2(H_2O)_2]\cdot 2DMF\cdot Et_2O$ (**1**) was synthesized with compartmental Schiff base ligand. The complex consists of a tetranuclear metallic core through the combination of crystallographic independent unit and its symmetry inversion containing four nickel ions arranged in linear. Ligand L^{2-} exhibits two coordination modes in the complex. Magnetic susceptibility measurement reveals that an antiferromagnetic interaction between the Ni(II) ions was observed in complex **1**, through two phenoxide oxygen atoms and three −N−N− bridging moieties.

ACKNOWLEDGMENTS

Supplementary material

Crystallographic data for structure **1**, described in this article has been deposited with the Cambridge Crystallographic Data Centre, CCDC Nos. 2384265, which can be obtained freely via E-mail: deposit@ccdc.cam.ac.uk or www: http://www.ccdc.cam.ac.uk, or by contacting The Cambridge Crystallographic Data Centre, 12 Union Road, Cambridge CB2 1EZ, UK; fax: +44 1223 336033.

REFERENCES

1. Lv, W.; Han, S.-D.; Li, X.-Y.; Wang, G.-M. Coordination chemistry and magnetic properties of polynuclear metal clusters/ cluster-based frameworks with tripodal alcohol ligands. *Coord. Chem. Rev.* **2023**, 495, 215376.
2. Matheson, B.E.; Dais, T.N.; Donaldson, M.E.; Rowlands, G. J.; Plieger, P.G. The importance of second sphere interactions on single molecule magnet performance. *Inorg. Chem. Front.* **2023**, 10, 6427-6439.
3. Chaudhry, M.T.; Akine, S.; MacLachlan, M.J. Contemporary macrocycles for discrete polymetallic complexes: precise control over structure and function. *Chem. Soc. Rev.* **2021**, 50, 10713-10732.
4. Georgiev, M.; Chamati, H. Fine structure and the huge zero-field splitting in Ni^{2+} complexes. *Mol.* **2022**, 27, 8887.
5. Song, W.; Wang, B.; Guo, K.; Zhang, W. Structures and magnetic properties of Nin (n = 36-40) clusters from first-principles calculations. *J. Struct. Chem.* **2016**, 57, 868-874.
6. Bonanno, N.M.; Lough, A.J.; Lemaire, M.T. A trinuclear nickel(II) cluster containing a ditopic redox active ligand: Structural and magnetic properties. *Polyhedron* **2020**, 183, 114536.
7. Su, Y.-M.; Ji, B.-Q.; Shao, F.; Zhang, S.-S.; Jagodič, M.; Jagličić, Z.; Gao, Z.-Y.; Dou, J.-M.; Sun, D. Carboxylic acid-tuned nickel(II) clusters: Syntheses, structures, solution behaviours and magnetic properties. *Dalton Trans.* **2021**, 50, 4355-4362.
8. Payne, E.H.; Wilson, L.R.B.; Singh, M.K.; Nichol, G.S.; Stewart, J.R.; Garcia-Sakai, V.; Ewings, R.A.; Lane, H.; Schnack, J.; Stock, C.; Brechin. E.K. Magnetic exchange, anisotropy and excitonic fluctuations in a $[Ni^{II}_7]$ Anderson wheel. *Inorg. Chem. Front.* **2024**, 11, 515.
9. Li, N.-F.; Wang, Q.; Li, J.-N.; Yu, Y.-T.; Xu, Y. Two SiO_4^{4-}-templated $Ln_{23}Ni_{20}$ clusters with magnetic cooling and stability. *Inorg. Chem.* **2022**, 61, 7180-7187.
10. Wang, L.; Wu, J.; Su, X.; Huang, J.; Zhang, P.; Zhao, S.; Su, B.; Xu, B. A linear tetranuclear Ni(II) acyl hydrazone Schiff base complex: preparation, crystal structure and catalytic application. *Transit. Metal Chem.* **2022**, 47, 275-281.
11. An, Z.-W.; Gao, Y.-Q.; Xu, S.-M.; Zhang, W.; Yao, M.-X. 3d ion-driven hexanuclear heterometallic clusters with amazing structures and magnetic properties. *Cryst. Growth Des.* **2023**, 23, 1412-1421.
12. Mahapatra, T.S.; Roy, B.C.; Dutta, B.; Lengyel, J.; Shatruk, M.; Ray, D. Structures and magnetic properties of a trinuclear angular $[Ni_3]$ and a heptanuclear wheel-like $[Ni_7]$ complexes with a Schiff base ligand. *Polyhedron* **2024**, 249, 116782.
13. Huang, X.R.; Yang, L.; Zhou, Y.-J.; Zhang, S.-h.; Zhang, H.Y.; Hai, H. Two linear trinuclear clusters based on Schiff base: Syntheses, structures and magnetic properties. *J. Clust. Sci.* **2015**, 26, 2033-2042.
14. Lin, P.-H.; Burchell, T.J.; Ungur, L.; Chibotaru, L.F.; Wernsdorfer, W.; Murugesu, M. A polynuclear lanthanide single-molecule magnet with a record anisotropic barrier. *Angew. Chem. Int. Ed.* **2009**, 48, 9489-9492.
15. Zou, L.-F.; Zhao, L.; Guo, Y.-N.; Yu, G.-M.; Guo, Y.; Tang, J.; Li, Y.-H. A dodecanuclear heterometallic dysprosium–cobalt wheel exhibiting single-molecule magnet behaviour. *Chem. Commun.* **2011**, 47, 8659-8661.

16. Huang, W.; Huang, S.; Zhang, M.; Chen, Y.; Zhuang, G.-L.; Li, Y.; Tong, M.-L.; Yong, J.; Li Y.; Wu, D. Multifunctional luminescent magnetic cryocooler in a Gd_5Mn_2 pyramidal complex. *Chem. Commun.* **2018**, 54, 4104-4107.
17. Sahu, M.; Manna, A.K.; Patra, G.K. A fluorescent colorimetric vanillin di-Schiff base chemosensor for detection of Cu(II) and isolation of trinuclear Cu(II)-dihydrazide. *Mater. Adv*. **2022**, 3, 2495-2504.
18. *Bruker APEX2, SAINT, SADABS*. Bruker AXS Inc. Madison: Wisconsin, USA; **2007**.
19. Sheldrick, G.M. SHELXT - Integrated space-group and crystal-structure determination. *Acta Cryst*. **2015**, A71, 3-8.
20. Hübschle, C.B.; Sheldrick, G.M.; Dittrich, B. ShelXle: A Qt graphical user interface for SHELXL. *J. Appl. Cryst.* **2011**, 44, 1281-1284.
21. Zhao, R.-X.; Wang, J.; Jing, D.-W.; Zhang, H.-J.; Feng, C.; Li, G.-Y. Syntheses, crystal structure and property of a heptanuclear cluster. *Inorg. Chem. Commun.* **2020**, 111, 107597.
22. Wu, J.; Zhao, L.; Zhang, P.; Zhang, L.; Guo, M.; Tang, J. Linear 3d-4f compounds: Synthesis, structure, and determination of the d-f magnetic interaction. *Dalton Trans.* **2015,** 44, 11935-11942.
23. Cindric, M.; Pavlovic, G.; Pajic, D.; Zadro, K.; Cincic, D.; Hrenar, T.; Leksic, E.; Prieto, A.B.P.; Lazic, P.; Jung, D.S. Correlation between structural, physical and chemical properties of three new tetranuclear Ni[II] clusters. *New J. Chem.* **2016**, 40, 6604-6614.
24. Chowdhury, T.; Adhikary, A.; Roy, M.; Zangrando, E.; Samanta, D.; Das, D. Mapping of solvent-mediated molecular self-assembly of iron(III) discrete compounds: exploring their magnetic behavior and phosphatase-like activity. *Cryst. Growth Des.* **2020**, 20, 1254-1265.
25. Chakarawet, K.; Atanasov, M.; Marbey, J.; Bunting, P.C.; Neese, F.; Hill, S.; Long, J.R. Strong electronic and magnetic coupling in M_4 (M = Ni, Cu) clusters via direct orbital interactions between low-coordinate metal centers. *J. Am. Chem. Soc.* **2020**, 142, 19161-19169.
26. Luo, R.; Xu, C.-G.; Tong, J.-P.; Shi, H.-Y.; Kong, X.-J.; Fan, Y.-H.; Shao, F. Synthesis, structure, and magnetism of a novel series of trinuclear nickel(II) clusters. *Cryst. Eng. Comm.* **2022**, 24, 5987-5994.
27. Xu, Y.; Hu, Z.-B.; Wu, L.-N.; Li, M.-X.; Wang, Z.-X.; Song, Y. Ferrimagnetic Fe(IV)-Mn(II) staircase chain constructed from Fe(IV) building block. *Polyhedron 2020, 175, 114243*.
28. Xu, Y.; Wu, L.-N.; Li, M.-X.; Shi, F.-N.; Wang, Z.-X. Syntheses, crystal structures and magnetic properties of two 1D copper complexes with Fe(IV) building block. *Inorg. Chem. Commun.* **2020**, 117, 107950.
29. Cao, C.; Liu, S.-J.; Yao, S.-L.; Zheng, T.-F.; Chen, Y.-Q.; Chen, J.-L.; Wen, H.-R. Spin-canted antiferromagnetic ordering in transition metal-organic frameworks based on tetranuclear clusters with mixed V- and Y-shaped ligands. *Cryst. Growth Des.* **2017**, 17, 4757-4765.